Carbohydrate Polymers 247 (2020) 116746

Contents lists available at ScienceDirect

Carbohydrate Polymers

journal homepage: www.elsevier.com/locate/carbpol

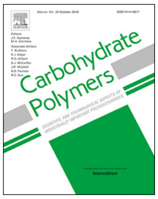

Ionic liquids facilitated dispersion of chitin nanowhiskers for reinforced epoxy composites

Jintian Wang[a], Zhiqiang Chen[a,b], Aaron (Qi) Guan[c], Nicole Raymonde Demarquette[d], Hani E. Naguib[e,*]

[a] *Department of Mechanical and Industrial Engineering, University of Toronto, 5 King's College Street, Toronto, Ontario, Canada*
[b] *State Key Lab for Strength and Vibration of Mechanical Structures, Department of Engineering Mechanics, Xi'an Jiaotong University, Xi'an, 710049, China*
[c] *BOCO Bio-Nanotechnologies Inc., 40 Pullman Court, Toronto, Canada*
[d] *École de Technologie Supérieure (ÉTS), Mechanical Engineering Department, 1100, rue Notre-Dame Ouest, Montréal, Québec, H3C 1K3, Canada*
[e] *Department of Mechanical and Industrial Engineering, Department of Materials Science and Engineering, Institute of Biomaterials and Biomedical Engineering, University of Toronto, 5 King's College Street, Toronto, Ontario, Canada*

ARTICLE INFO

Keywords:
Chitin nanowhiskers
Ionic liquids
Nanofiller dispersion
Mechanical properties
Nanocomposites

ABSTRACT

In this work, we propose a novel approach to produce a high-strength epoxy nanocomposite using ionic liquids facilitated dispersion of chitin nanowhiskers (CNWs). Samples with 0 – 3 wt% CNWs and 1 wt% of [Emim][OAc] were fabricated by mixing, casting, and curing. The morphological observations of the ethanol/ionic liquid suspensions by TEM indicated that [Emim][OAc] helped in dispersing the CNWs. The tensile, impact, dynamical mechanical properties, and thermal stability of the composites were further evaluated to access the reinforcing effect of CNWs. Increase of 35 % tensile strength, 175 % toughness and 90 % impact strength were observed upon addition of 2 wt% of CNWs. Thermal stability of the epoxy was not affected by the addition of CNWs. The SEM observations of the composites evidenced that the fracture mechanisms had changed upon CNWs addition. This work shows the advantage of the novel approach using ionic liquids as nanofiller dispersant in fabricating CNWs nanocomposites.

1. Introduction

Nanocomposites have garnered tremendous attention of both industry and academia for either their enhanced mechanical strength[1], electrical conductivity, thermostability or sustainability. To date, several types of nanofillers, such as carbon nanotubes, graphene nanoplatelets, nanoclays and nanocellulose, have been added to various polymers to obtain nanocomposites (Anwer, Wang, & Naguib, 2019; Choi & Jeong, 2019; Feng, Xie, & Zhong, 2014; Miyagawa, Misra, & Mohanty, 2005; Radich, McGinn, & Kamat, 2011; Withers et al., 2015; Wu, Xie, Zhang, Jia, & Zhang, 2019; Zakaria et al., 2019). Among these nanofillers, chitin, a natural polymer, has been viewed as a very interesting material due to its natural abundance and mechanical properties that rival the ones of synthetic expensive nanofillers (Gopalan Nair & Dufresne, 2003a, 2003b; Nair, Dufresne, Gandini, & Belgacem, 2003). Chitin is a biopolymer that can be found in exoskeleton of crustacean, cuticle of insects, and cell walls of fungi. It is the second most abundant natural polymer after cellulose. The chitin molecule, which belongs to the polysaccharide family, presents different crystalline polymorphs including α-, β-, and γ-chitin depending on the sources (Kurita, 2001; Li, Revol, & Marchessault, 1997; Morin & Dufresne, 2002). α-chitin is the most abundant one and originates from crustacean shells, β-chitin is obtained from the pen of squids (Fan, Saito, & Isogai, 2008; Ifuku et al., 2009; Jang, Kong, Jeong, Lee, & Nah, 2004) and γ-chitin, the least abundant can be found in the stomach of Loligo. In general, chitin molecules are very rigid, group themselves in a parallel fashion, adopting a molecular conformation that will vary according to the type of crystals (α, β or γ). These assemblies of parallel chains are arranged to form sheets which further wrap up to rod-like structures with a length of 200 – 500 nm and a diameter of 10 – 20 nm resulting in so-called chitin nanowhiskers (CNWs) (Blackwell, 1969). Chitin nanowhiskers (CNWs) present a high modulus of 200 GPa and large aspect ratio, making them good candidates for potential usage for mechanical reinforcement in nanocomposites (Chen et al., 2018; Guo, Duan, Cui, & Zhu, 2015; Jun et al., 2020; Liu, Liu, Yang, Luo, & Zhou, 2018; Zhou et al., 2015). However, and independent of the crystalline

---

* Corresponding author.
E-mail addresses: jintian.wang@mail.utoronto.ca (J. Wang), zq.chen@mail.utoronto.ca (Z. Chen), aaron.guan@bocotechnology.com (A.Q. Guan), nicoler.demarquette@etsmtl.ca (N.R. Demarquette), naguib@mie.utoronto.ca (H.E. Naguib).

https://doi.org/10.1016/j.carbpol.2020.116746
Received 11 May 2020; Received in revised form 6 July 2020; Accepted 8 July 2020

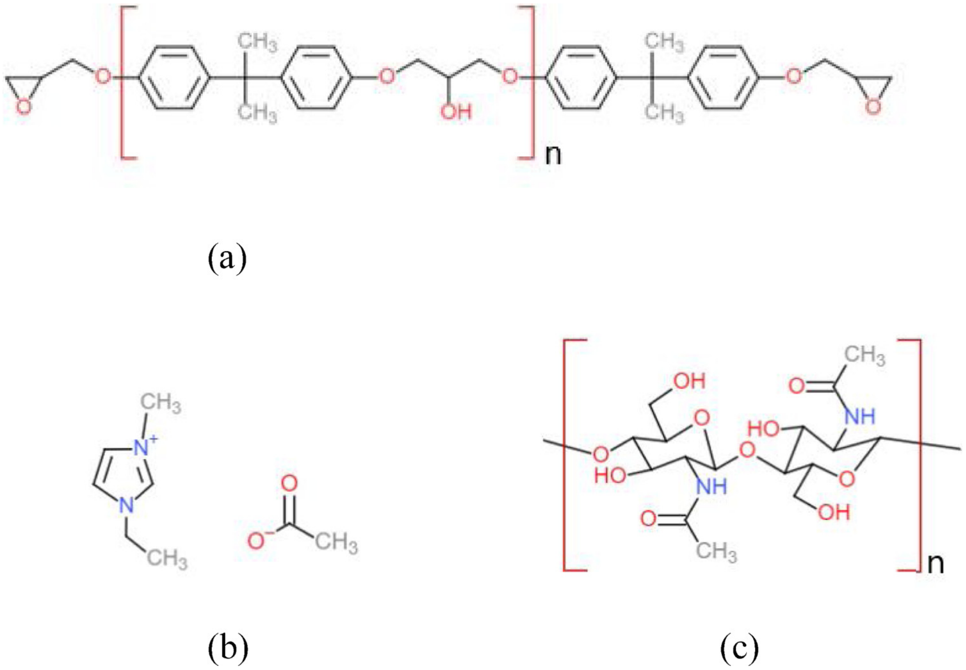

Scheme 1. Chemical structures of DGEBA, [Emim][OAc] and chitin.

structure in which they are involved, chitin molecules are closely linked via hydrogen bonding resulting in a very poor solubility in most common solvents and very difficult dispersion in polymeric systems (Araki & Kurihara, 2015; Coltelli et al., 2019; Zhang, Wei, Huang, Feng, & Chang, 2014) These links are even stronger in the case of α-chitin because of the conformation adopted by the polymer chains within the crystals turning the dispersion of this nanofiller a challenging problem if one wants to harness the properties that these fillers could impart to the composite.

Chitin nanocomposites that incorporating chitin nanofillers into diverse matrix such as sorbitol polyglycidyl ether (SPE), poly (vinyl alcohol) PVA and thermoset DGEBA epoxy resin (Anwer, Wang, Guan, & Naguib, 2019; Irvin, Satam, Carson Meredith, & Shofner, 2019; Shibata, Enjoji, Sakazume, & Ifuku, 2016) have been successfully obtained by several authors. However, limited improvement on mechanical properties, upon addition of chitin were observed. In some cases, it has even been observed that the addition of chitin resulted in a decrease of mechanical of properties (Shibata et al., 2018). For that reason chitin nanofibers have been considered inadequate to reinforce high tensile strength (40 MPa) cured resins although previous results of our group showed that the addition of chitin could result in an increase of tensile strength of epoxy resin with around 70 MPa (Anwer, Wang, Guan et al., 2019). The underperformance of the composites obtained was often attributed to the excessive agglomeration of CNWs as chitin was merely dispersed in the solution during the fabrication process. Proper strategies to disperse CNWs within the solution to be polymerized should therefore be explored.

Multiple dispersion methods have been developed over the years, including sonication and addition of dispersant (Anwer, Wang, & Naguib, 2019; Gao et al., 2019; Kumar, Ghosh, Yadav, & Kumar, 2017; Li, Gao, Zhao, Sun, & Li, 2017). More recently, ionic liquids have been reported as an effective dispersant especially for carbon-based nanomaterials (Fukushima et al., 2006; Lu, Yan, & Texter, 2009; Sanes, Saurín, Carrión, Ojados, & Bermúdez, 2016; Shamsuri & Daik, 2015; Xiang, Suo, Xu, & Hu, 2018; Yousfi, Livi, & Duchet-Rumeau, 2014). As an example, they have been used successfully to disperse silica in rubber (Donato, Donato, Schrekker, & Matějka, 2012), (resulting in materials with improved toughness), nanotubes (Hameed et al., 2013) and graphene (Liu, Qiu, Du, Zhao, & Wang, 2018) to obtain conductive nanocomposites. Ionic liquids are organic salts whose melting points are below a certain temperature (usually about 100 °C) resulting from the poor coordination of their constituting ions. They are known for their excellent thermal and chemical stability and non-flammability. They have been used as processing media for dissolving and regenerating chitin (Wu, Sasaki, Irie, & Sakurai, 2008). However, we could not find any report in the literature, which used ionic liquids to disperse chitin within polymers. Although chitin nanowhiskers has outstanding mechanical properties and great potential for composites reinforcement, the intrinsic agglomeration of chitin results in the harness of such properties still challenging as mentioned. In this study, chitin epoxy composites were obtained adding ionic liquid to a CNWs suspension within DGEBA resulting in a liquid material that was further cured. 1-Ethyl-3-methylimidazolium acetate, an imidazolium ionic liquid denoted as [Emim][OAc] was chosen because it has been shown that it could be a good candidate to dissolve chitin (Qin, Lu, Sun, & Rogers, 2010). With the capability of dissecting chitin molecules, [Emim][OAc] applied to CNWs in polymer matrix may play an important role for chitin nanofiller dispersion. We hypothesize that the interaction between [Emim][OAc] and chitin may diminish chitin's intrinsic agglomeration and thus facilitate the CNWs dispersion in epoxy composites for improved mechanical properties. The composites were tested for their mechanical as well as thermal properties which were correlated to their morphology. A phenomenological model explaining the interactions between the components of the composites was then proposed.

2. Materials and methods

2.1. Materials

The ionic liquid 1-Ethyl-3-methylimidazolium acetate ([Emim][OAc]) was purchased from Ionic Liquids Technologies Gmbh (Heilbronn, Germany) with the 1-Ethyl-3-methylimidazolium and acetate content over 99.3 % and 99.9 % respectively. This ionic liquid was chosen for its ability to properly disperse chitin, and its functional groups that enable the curing of epoxy (Zhou, Mingyuan, Jin, & Wang, 2005). The chitin nanowhiskers (CNWs) (specific surface area of 200 − 300 mˆ2/g and aspect ratio of 20–50) used with the same polymorphs as that has been previously reported (Anwer, Wang, Naguib, Naguib et al., 2019; Chi-Yan Li, Sun, Guan, & Naguib, 2016) were obtained from BOCO Technology (Ontario, Canada) in the form of ethanol suspension. The weight concentration of CNWs was 8 wt% as confirmed by TGA. The epoxy resin EPON828, a high purity type of DGEBA obtained by reaction of epichlorohydrin and bisphenol A, was purchased from Hexion (Ohio, United States). All chemicals listed were used as received without further purification.

Schemes 1 (a–c) present the chemical structures of the DGEBA, [Emim][OAc], chitin nanowhiskers that used in the present work.

2.2. Fabrication methodology

The CNWs ethanol suspension was first characterized by TGA (Q50 TA Instrument) to measure the solid content of CNWs. For that the samples were heated at a temperature of 150 °C which was held constant for 20 min. To obtain the composites samples, the CNWs ethanol suspension containing the desired amount of CNWs was added dropwise to the DGEBA epoxy, the mixture was stirred at 300 rpm for at least 5 h at a temperature of 70 °C for all the ethanol to evaporate. A transparent epoxy chitin suspension was then obtained. The ethanol volatile content leftover was confirmed using TGA to be less than 0.5 % with respect to the amount of epoxy. Afterward, [Emim][OAc] was added to the uniform chitin epoxy suspension. The mixture was then stirred at 100 rpm at a temperature 50 °C until a homogeneous liquid was obtained. The solution was degassed in a vacuum chamber for 30 min to remove the air bubbles and then casted in customized two-part rectangular glass molds to a sheet. The solution was prevented from oxidation and placed in an oven at 100 °C for 24 h to complete the cure. The reaction mechanism between epoxy resin with imidazoles has been examined by some previous literature and is presented in Scheme 2 (Binks, Cavalli, Henningsen, Howlin, & Hamerton, 2018; Bodnar, Hartmann, & Borbely, 2005; Ham et al., 2010; Jíšová, 1987; Maka, Spychaj, & Pilawka, 2012; Vashchuk, Fainleib, Starostenko, & Grande, 2018). The imidazole groups, under heating condition, tend to open up the epoxy ring and induce the etherification of epoxy resin to form stable compounds that polymerize with sufficient epoxide groups. For the neat epoxy composites without CNWs, the whole process just skipped the CNWs ethanol suspension mixing step. The completion of curing and the stability of the composites were further confirmed with no mass loss or ILs leaching after solvent treatment by water, ethanol, acetone and dimethylformamide. Laser cutting was used to obtain various specimens according to each testing standard. The concentration of [Emim][OAc] was kept constant as 1 wt% for samples with different CNWs loadings in DGEBA. Table 1 summarizes the naming policy for all nanocomposites fabricated in this study.

2.3. Morphological characterization

The CNWs ethanol suspensions with or without ionic liquids were dried and loaded on CF200-Cu grids. They were further observed by TEM using a FEI Tecnai 20 TEM (magnification x200k) (Field Electron and Ion (FEI) company, Hillsboro, Oregon). These observations were carried out to investigate the dispersing effect of the [Emim][OAc]. The fractures of the composites were obtained by 5 min of immersion in liquid nitrogen followed by mechanical breaking and then sputter coated and carbon pasted. Their morphology was observed by SEM using a JEOL JSM 1000 SEM (magnification x15k) (JSM USA, Inc., Peabody, Massachusetts).

Table 1
Designation of [Emim][OAc], CNWs and DGEBA nanocomposites and corresponding composition used.

Designation	wt% [Emim][OAc]	wt% CNWs	wt% DGEBA
Neat	1	——	99
0.75 wt%	1	0.75	98.25
1 wt%	1	1	98
1.5 wt%	1	1.5	97.5
2 wt%	1	2	97
3 wt%	1	3	96

2.4. Tensile testing

Tensile tests were carried out according to the ASTM standard D638 using a Universal Testing Machines Instron 5848 (Instron, Norwood, Massachusetts). Samples were laser cut to dumbbell shape following the TypeV specimen dimensions and the loading rate was set at 5 mm/minute.

2.5. Impact testing

Impact tests were performed using impact tester Instron Dynatup (Instron, Norwood, Massachusetts) following ISO179 standard. The Type I charpy flatwise samples were laser cut to bar shape with the dimension of 80 mm (L) x10 mm (W) x3 mm (T). The span, namely the distance between supporting and clamping, was set as 62 mm accordingly. The average impact speed of 4.5 lb impact mass was about 1.7 m/s which was adequate to induce complete fracture of specimens. The Charpy impact strength, expressed in kilojoules per square meter, was calculated with the following formula from the standard ISO179:

$$a_{cU} = \frac{E_c}{h*b}*10^3 \tag{1}$$

Where $\mathbf{E_c}$ *is the energy absorbed by the fracture specimens in joules, h is the thickness of the specimens in millimeters, b is the width of the specimens in millimeters*

2.6. Dynamic mechanical testing

Dynamic mechanical tests were performed using a dynamic mechanical analyzer DMA Q800 (TA Instruments, New castle, Delaware) with the dual cantilever setup under temperature ramp of 3 °C/min to 160.00 °C with constant strain of 0.01 % at a frequency of 1 Hz. The samples were prepared with the rectangular shape of 60 mm (L) x12 mm (W) x1.5 mm (T). The storage modulus, loss modulus and tan delta were recorded to analyze the glass transition temperature.

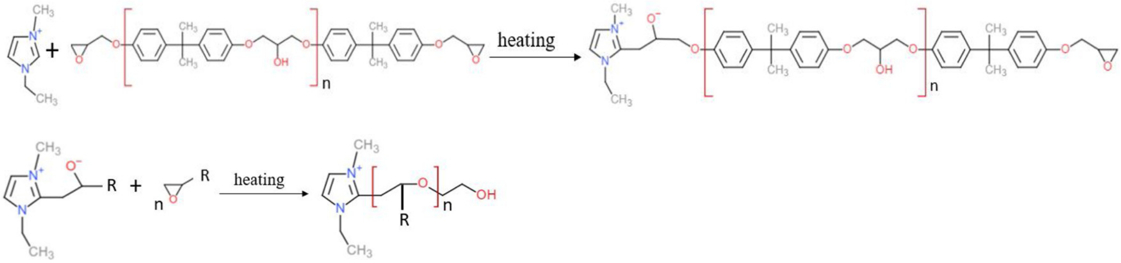

Scheme 2. Curing mechanism of epoxy resin with imidazolium ionic liquids [Emim][OAc].

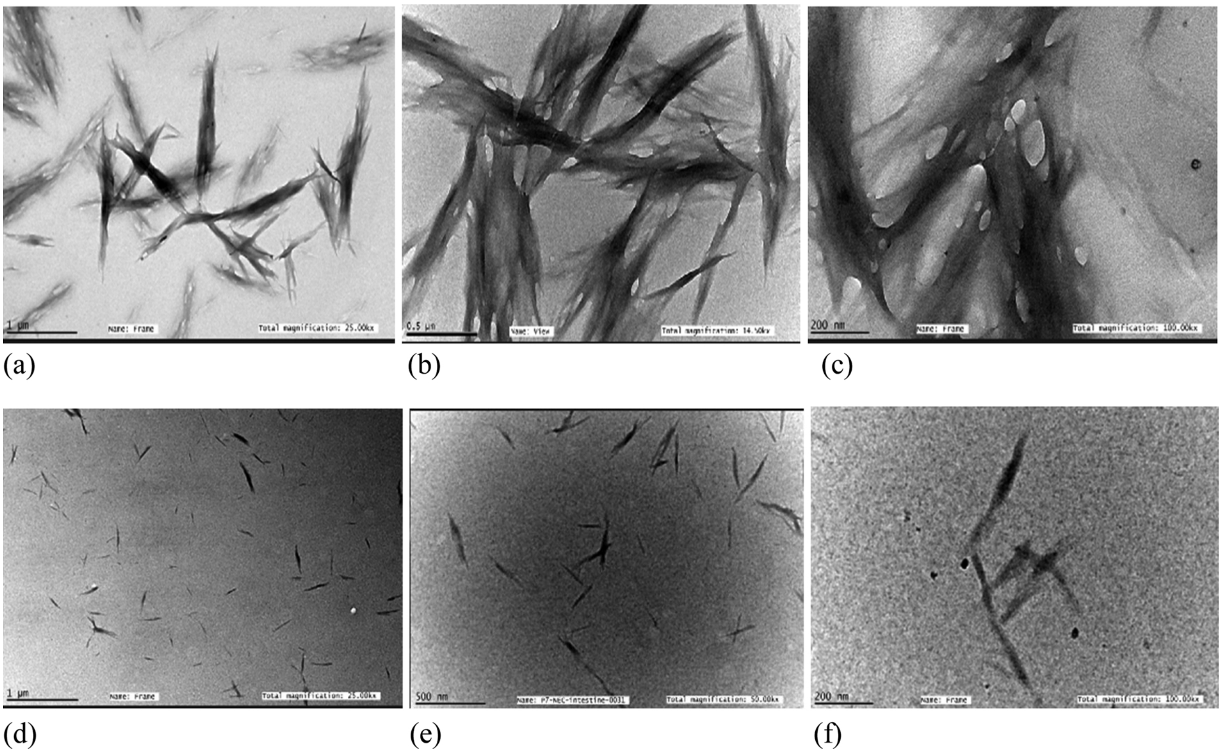

Fig. 1. CNWs morphology characterization under TEM: (a-c) images of CNWs untreated with [Emim][OAc] in which scale bars are 1 μm, 0.5 μm and 200 nm, respectively (d-f) images of CNWs treated with [Emim][OAc] in which scale bars are 1 μm, 500 nm and 200 nm, respectively.

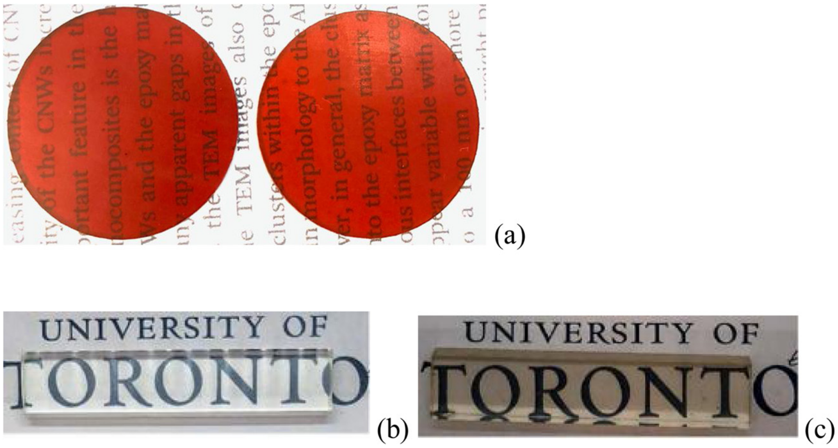

Fig. 2. (a) [Emim][OAc] cured epoxy (left) and [Emim][OAc] cured epoxy with 3 wt% CNWs (right) (b) TETA cured neat epoxy (c) TETA cured epoxy with 0.75 wt% CNWs.

2.7. *Thermogravimetric analysis*

The thermal stability of the nanocomposites was studied via thermogravimetric analysis TGA Q500 (TA Instruments, New castle, Delaware). Samples less than 50 mg were cut from the sheets and loaded on a platinum plate. The full cycle of testing had the temperature ramped from room temperature to 1000 °C at the rate of 20 °C/minute under nitrogen environment.

3. Results

3.1. *CNWs morphology and composites appearance*

CNWs morphology and composites appearance. Fig. 1 presents the typical aspects of chitin nanowhiskers ethanol suspension to which [Emim][OAc] were not (Fig. 1a–c) or were added (Fig. 1d–f). Figures with different magnification from x25k to x100k are presented for clarification. The mass ratio of CNWs and [Emim][OAc] concentration for the micrographs shown Fig. 1d–f is 2:1. It can be seen that upon addition of [Emim][OAc], the size of the aggregates of CNWs decreases tremendously, indicating that the [Emim][OAc] could play a role in dispersing the fibers within the DGEBA. Fig. 2a shows the ruby appearance of both [Emim][OAc] cured neat epoxy samples (on the left) and samples with 3 wt% CNWs. For comparison, neat epoxy cured with amine hardener triethylenetetramine (TETA) (Fig. 2b) and that with 0.75 wt% CNWs (Fig. 2c) from our previous study are presented (Anwer, Wang, Guan et al., 2019). Neat epoxy sample cured with TETA is absolute transparent while the addition of CNWs leads to the brownish appearance. In addition, the testing results from our previous study have demonstrated the occurrence of chitin agglomeration at 0.75 wt%. However, for [Emim][OAc] cured samples, there is no difference observed between neat samples and that with 3 wt% CNWs.

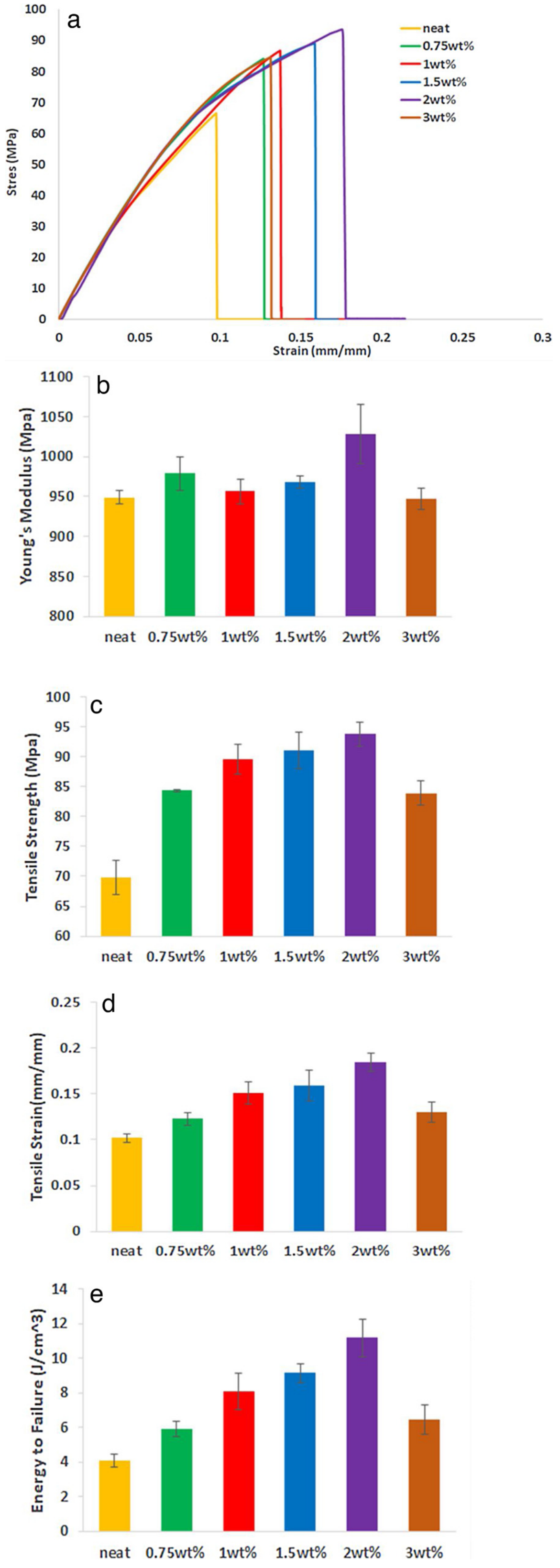

Fig. 3. Tensile mechanical properties: (a) stress-strain curves (b) Young's modulus (c) tensile strength (d) tensile strain (e) energy to failure.

Also, our previous studies also showed that it was impossible to disperse adequately chitin in DGEBA once the concentration was above 0.75 wt % as the viscosity was too high. These observations further indicate that the EmimAc helps in the dispersion of CNWs with the epoxy.

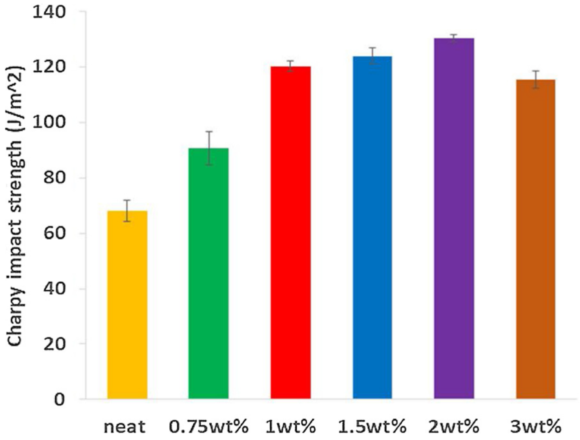

Fig. 4. Charpy impact properties of the nanocomposites.

3.2. Mechanical and impact properties

Fig. 3 presents the mechanical properties as extracted from tensile data of the composites obtained in this work. Fig. 4 presents their impact properties. The statistical comparison of both mechanical and impact properties is presented in Table 2 as specific values with standard deviation. It can be seen that the addition of CNWs results in an improvement of mechanical properties for concentrations of up to 2 wt % CNWs. The addition of 2 wt% CNWs resulted in an increase of modulus of 8%, tensile strength of 35 %, strain of 80 %, energy to failure of 175 % increase and 90 % increase of impact strength. These increases are much larger than the ones that were obtained in our previous work. It was shown that when CNWs were incorporated in TETA cured epoxy from 0.25 wt% to 0.75 wt%, the optimal properties were achieved at 0.25 wt% CNWs loadings with Young's modulus, tensile stress and energy to failure increasing by 23 %, 12 %, and 2.5 % respectively (Anwer, Wang, Guan et al., 2019). Furthermore, when CNWs was added to TETA cured epoxy, the increase of tensile strength was accompanied with a decrease of tensile strain and impact strength. This was attributed to a worse dispersion of CNWs within the epoxy and was supported by corresponding SEM and TEM images. However, when [Emim][OAc] was used, all mechanical properties are increasing. The increase of tensile strength is not accompanied by the decrease of tensile strain as is normally observed when one adds fillers to a polymer. Interestingly, the Young modulus of the composites did not increase much upon addition of CNWs which is unexpected as chitin presents a much higher tensile modulus than the epoxy. This could be attributed to a plasticizing effect of the ionic liquid in thermoset materials[37]. The presence of the ionic liquid could therefore offset the influence of CWN. For concentrations of CWN of 3 wt% a decrease of all mechanical properties is observed. Causes to explain this phenomenon will be further addressed in the discussions. Furthermore, the chitin agglomeration limited the CNWs loading to 0.75 wt% in the manner of sample fabrication of TETA cured epoxy. However, it was possible to incorporate up to 3 wt% CNWs when [Emim][OAc] was used.

3.3. Surface morphology of the composites

Fig. 5 presents the scanning electron micrographs of the cryo-fractures of the pure epoxy composites and of 5 composites that were obtained with the addition of [Emim][OAc] with 0.75, 1, 1.5, 2, 3 wt% CNWs. Figures are presented with the magnification of x5k and all scale bars of 5 μm for comparison. It can be seen that upon addition of CNWs, the fracture surface of the samples is altered. Whereas in the case of the neat epoxy the plastic deformation of the matrix dominated the fracture

Table 2
Statistical comparison of the mechanical properties and impact properties.

Designation	Young's modulus (MPa)	Tensile strength (MPa)	Tensile strain (mm/mm)	Energy to failure (J/cm^3)	Impact strength (J/m^2)
Neat	948.83 ± 8.70	69.76 ± 2.93	0.10 ± 0.0048	4.07 ± 0.36	68.17 ± 3.83
0.75 wt%	978.92 ± 20.89	84.33 ± 0.17	0.12 ± 0.0067	5.90 ± 0.43	90.70 ± 6.07
1 wt%	956.33 ± 15.28	89.59 ± 2.47	0.15 ± 0.012	8.08 ± 1.08	120.44 ± 1.93
1.5 wt%	967.62 ± 7.93	91.08 ± 3.09	0.16 ± 0.017	9.14 ± 0.55	124.03 ± 2.84
2 wt%	1028.06 ± 37.31	93.80 ± 2.06	0.18 ± 0.0098	11.18 ± 1.08	130.48 ± 1.21
3 wt%	946.70 ± 13.34	83.92 ± 2.00	0.13 ± 0.011	6.43 ± 0.85	115.48 ± 3.08

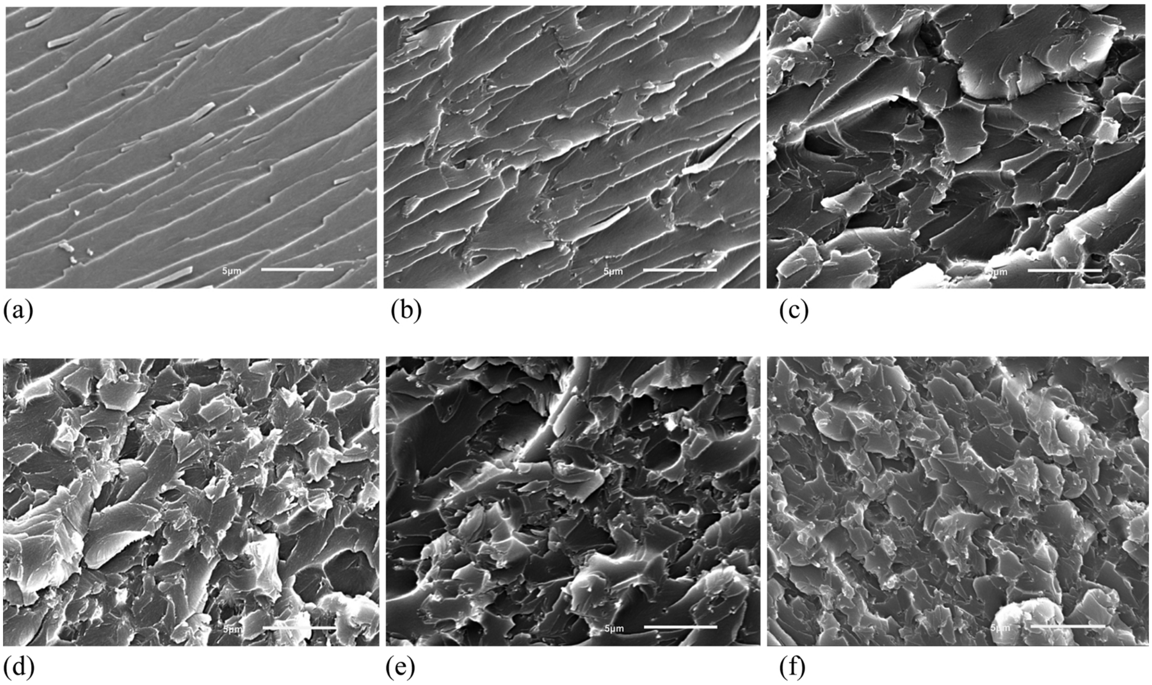

Fig. 5. SEM images of the cryofracture surface of the nanocomposites: (a) neat (b) 0.75 wt% CNWs (c) 1 wt% CNWs (d) 1.5 wt% CNWs (e) 2 wt% CNWs (f) 3 wt% CNWs in which scale bars are all 5 μm.

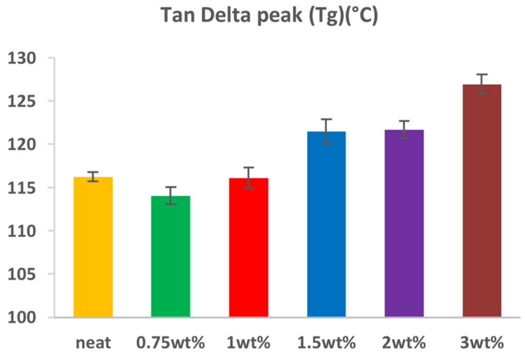

Fig. 6. Glass transition temperature of the composites obtained in this work.

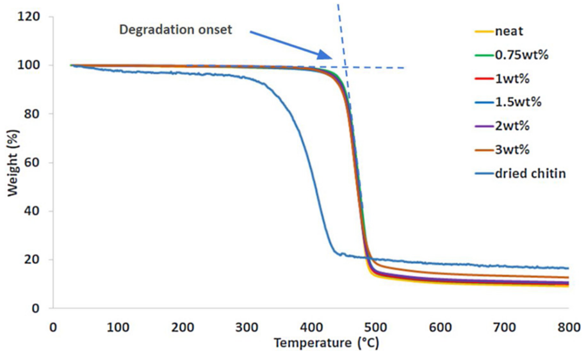

Fig. 7. Thermogravimetric analysis of the samples studied in this work.

behavior and granted most of the impact strength, the addition of CNWs suddenly altered the fracture surface with sags and crests caused by the fiber debonding. This fiber debonding could be at the origin of this improvement of impact strength. The energy dissipation of fiber pullout and breaking might be insignificant since the size and aspect ratios of CNWs constrained their participation in major crack propagation (Kausar & Taherian, 2019; Suo, 1992). With the concentration of CNWs increasing, the fracture surfaces showed denser sags and crests implying that more fiber debonding happened in a certain interfacial region. These results indicate that fiber debonding could be at the origin of the increased impact strength. The SEM images of cryofracture features for the TETA cured epoxy with or without CNWs from our previous study had shown similar trend of morphologies change. The only difference that was observed was a poorer dispersion of the chitin fibers in the case of a composite to which 0.75 wt% chitin fibers had been added (Anwer, Wang, Guan et al., 2019).

3.4. Thermal properties

Fig. 6 presents the glass transition temperatures of the different composites obtained in this work evaluated by DMA. It can be seen that upon addition of CNWs, the glass transition temperature increased for concentrations of CNWs above 1 wt% probably as a result of the chain

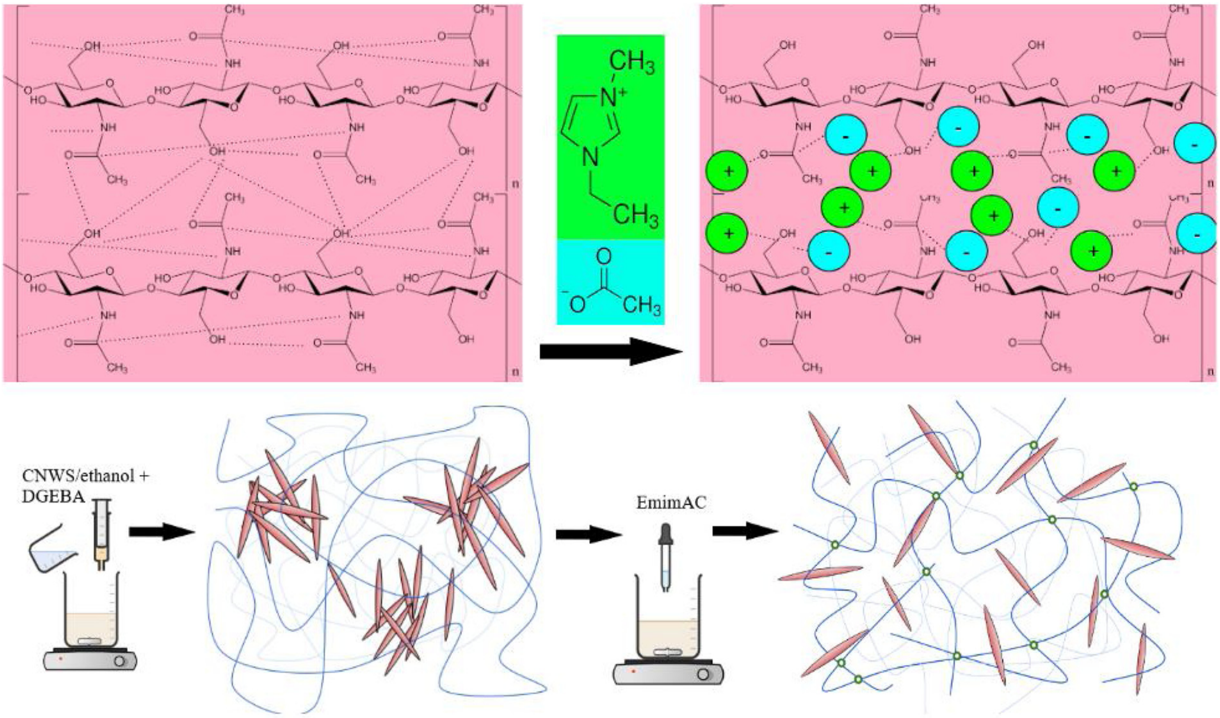

Fig. 8. Chemical scheme explaining the dispersing role of the ionic salt.

mobility hindrance brought by the presence of CNWs. Although no chemical reaction occurred between CNWs and the epoxy (as confirmed by FTIR (Anwer, Wang, Guan et al., 2019)) the functional groups of chitin and epoxy probably form hydrogen bonds and induce intermolecular forces that restrain the mobility of epoxy polymer chains. The glass transition temperatures of the composites obtained in this work in the presence of [Emim][OAc], are lower than the ones for composites cured with TETA (Anwer, Wang, Guan et al., 2019). This difference probably originates from the plasticizing effect of [Emim][OAc]. Initially, as the amount of [Emim][OAc] offset that of epoxy when 0.75 wt% CNWs added, the glass transition temperature dropped compared with neat [Emim][OAc] cured epoxy. Afterward, the hinderance of chain mobility from CNWs surpassed the plasticizing effect of [Emim][OAc], the glass transition temperature increased with the CNWs concentration.

Fig. 7 shows the mass loss as a function of temperature for the dried chitin, pure epoxy, and composites. Thermal stability and degradation analysis were performed via thermogravimetric analysis (TGA) for the nanocomposites. Dried chitin was prepared via direct drying of chitin ethanol suspension. The initial weight loss of dried chitin at 10 wt% around 200 °C was considered trapped volatile content within the CNWs structure. After that, there was a dramatic weight loss before 500 °C due to the decomposition of major polymer chains and side groups such as acetyl and methyl groups (Moussout, Ahlafi, Aazza, & Bourakhouadar, 2016). The final step of thermal degradation was ascribed to the destruction of pyranose ring and residual carbon (Corazzari et al., 2015; Marroquin, Rhee, & Park, 2013). Due to the small concentration of CNWs in the nanocomposites, the major thermal degradation behavior overall is almost the same as the cured epoxy matrix. There is slight difference shown on the weight residue as chitin itself would degrade less than the epoxy matrix would. The degradation onset (Fig. 7) was extrapolated by the major curve showing weight drop around 450 °C and was similar for samples with different concentrations of CNWs. Thus, the addition of CNWs did not influence the thermal stability of the nanocomposites in terms of thermal degradation.

4. Discussion

The experimental results obtained in this manuscript showed that a better dispersion of CNWs can be obtained when [Emim][OAc] is used in the preparation of epoxy CNWs composites. When [Emim][OAc] was used, the addition of CNWs did not result in a change of opacity of epoxy samples for concentration of CNWs of up to 3 wt%. Conversely, the addition of 0.75 wt% resulted in an increase of opacity of the sample when no ionic liquid was used. Furthermore, the use of ionic liquid enabled an increase of CNWs that can be added to the epoxy samples. The enhanced dispersion of the CNWs also resulted in more effective improvement of mechanical properties. However, the results indicated that the concentrations of [Emim][OAc] vs CNW added to the epoxy have to be optimized as once the CNWs increases above a certain value (namely 3 wt% in this work), the ionic salt was unable to disperse properly the CNWs. Both tensile and impact properties drew back at 3 wt% CNWs. This can probably be explained in terms of insufficient functional ionic salt functional groups that can help disrupting the abundant intra and intermolecular forces in CNWs effectively as will be explain by the phenomenological model below.

Fig. 8 proposed a possible interaction mechanism between the chitin, [Emim][OAc] and epoxy resin used in the present work. When the ionic liquid is added to the chitin suspension, it is expected that the anions of the chosen ionic liquid interact with the polar part domains of the chitin (Kadokawa, 2019) and intercalate between the chitin molecules. The ability of the salt to “break” the hydrogen bonds between the chitin molecules to intercalate between them and form new bonds with them can be attributed to the β-hydrogen bond basicity, an empirical solvent denotation for quantitative comparison of dissolubility (Yokoyama, Taft, & Kamlet, 1976) which in the case of the present salt is fairly high (Qin et al., 2010). These interactions between the chitin molecules and the salt could explain the ability of the later to disperse the chitin within the DGEBA epoxy. The dispersion was kept within the nanocomposite due to the ability of the ionic salt to cure the epoxy and resulted in transparent materials. Therefore, the treatment of appropriate ionic liquids on CNWs in nanocomposites facilitated the nanofiller dispersion and provided a new perspective for overcoming chitin’s intrinsic agglomeration in composites system for reinforcement.

Finally, the plasticizing effect of ionic liquids [Emim][OAc] competed with hinderance effect of CNWs on the polymer chain mobility. Thus, the glass transition of the composites dropped at 0.75 wt% but increased with higher concentration of CNWs from 1 wt% to 3 wt%. Moreover, the addition of CNWs did not influence the thermal stability of the composites.

5. Conclusion

Dispersion of chitin nanofillers is still a challenging problem, when producing nanocomposites, as they tend to agglomerate when added to the resin. This work first time exploited the unique capability of ionic liquids to separate chitin aggregation via intermolecular forces to disperse CNWs in epoxy matrix. This work confirmed the hypothesis that the treatment of a properly chosen ionic liquid on CNWs alleviated chitin's intrinsic agglomeration, allowing the dispersion of a larger concentration of nanofillers (3 wt% vs 0.75 wt%) within the polymer and greater improvement of mechanical properties. However, the ratio of the ionic liquid to CNWs should be optimized as the ionic liquid acts as a plasticizer of the resin. This paper has demonstrated the effective dispersion from ionic liquids for the bio-based nanofiller CNWs, expanding greatly the application potential of CNWs in other nanocomposites for reinforcement and the application of ionic liquids for dispersion of other biopolymers in composites system. Furthermore, the study has shown the reinforcement contributed by CNWs as nanofillers in epoxy composites, which provided a strong candidate for replacement of conventional nanofillers in epoxy industries.

CRediT authorship contribution statement

Jintian Wang: Conceptualization, Methodology, Validation, Formal analysis, Writing - original draft. **Zhiqiang Chen:** Methodology, Formal analysis. **Aaron (Qi) Guan:** Project administration. **Nicole Raymonde Demarquette:** Writing - review & editing. **Hani E. Naguib:** Conceptualization, Writing - review & editing, Supervision.

Declaration of Competing Interest

None.

Acknowledgments

The authors of this work would like to acknowledge the support from Mitacs Accelerate program (Grant number: IT13261). Zhiqiang Chen acknowledges the support from the China Scholarship Council (No. 201806280391).

References

Anwer, M. A. S., Wang, J., Guan, A., & Naguib, H. E. (2019). Chitin nano-whiskers (CNWs) as a bio-based bio-degradable reinforcement for epoxy: evaluation of the impact of CNWs on the morphological, fracture, mechanical, dynamic mechanical, and thermal characteristics of DGEBA epoxy resin. *RSC Advances*. https://doi.org/10.1039/C9RA00769E.

Anwer, M. A. S., Wang, J., & Naguib, H. E. (2019). 1D/2D CNF/GNP hybrid nanofillers: Evaluation of the effect of surfactant on the morphological, mechanical, fracture, and thermal characteristics of their nanocomposites with epoxy resin. *Industrial & Engineering Chemistry Research*. https://doi.org/10.1021/acs.iecr.9b00956.

Anwer, M. A. S., Wang, J., & Naguib, H. E. (2019). 1D/2D CNF/GNP hybrid nanofillers: Evaluation of the Effect of surfactant on the morphological, mechanical, fracture, and thermal characteristics of their nanocomposites with epoxy resin. *Industrial & Engineering Chemistry Research, 58*(19), 8131–8139. https://doi.org/10.1021/acs.iecr.9b00956 research-article.

Araki, J., & Kurihara, M. (2015). Preparation of sterically stabilized chitin nanowhisker dispersions by grafting of poly(ethylene glycol) and evaluation of their dispersion stability. *Biomacromolecules*. https://doi.org/10.1021/bm5016078.

Binks, F. C., Cavalli, G., Henningsen, M., Howlin, B. J., & Hamerton, I. (2018). Investigating the mechanism through which ionic liquids initiate the polymerisation of epoxy resins. *Polymer, 139*, 163–176. https://doi.org/10.1016/j.polymer.2018.01.087.

Blackwell, J. (1969). Structure of β-chitin or parallel chain systems of poly-β-(1→4)-N-acetyl-D-glucosamine. *Biopolymers*. https://doi.org/10.1002/bip.1969.360070302.

Bodnar, M., Hartmann, J. F., & Borbely, J. (2005). Preparation and characterization of chitosan-based nanoparticles. *Biomacromolecules, 6*(5), 2521–2527. https://doi.org/10.1021/bm0502258.

Chen, C., Deng, S., Yang, Y., Yang, D., Ye, T., & Li, D. (2018). Highly transparent chitin nanofiber/gelatin nanocomposite with enhanced mechanical properties. *Cellulose, 25*(9), 5063–5070. https://doi.org/10.1007/s10570-018-1915-z.

Chi-Yan Li, S., Sun, Y. C., Guan, Q., & Naguib, H. (2016). Effects of chitin nanowhiskers on the thermal, barrier, mechanical, and rheological properties of polypropylene nanocomposites. *RSC Advances, 6*(76), 72086–72095. https://doi.org/10.1039/c6ra11623j.

Choi, H. Y., & Jeong, Y. G. (2019). Microstructures and piezoelectric performance of eco-friendly composite films based on nanocellulose and barium titanate nanoparticle. *Composites Part B: Engineering, 168*, 58–65. https://doi.org/10.1016/J.COMPOSITESB.2018.12.072.

Coltelli, M. B., Cinelli, P., Gigante, V., Aliotta, L., Morganti, P., Panariello, L., … Lazzeri, A. (2019). Chitin nanofibrils in poly(Lactic acid) (PLA) nanocomposites: Dispersion and thermo-mechanical properties. *International Journal of Molecular Sciences, 20*(3), https://doi.org/10.3390/ijms20030504.

Corazzari, I., Nisticò, R., Turci, F., Faga, M. G., Franzoso, F., Tabasso, S., … Magnacca, G. (2015). Advanced physico-chemical characterization of chitosan by means of TGA coupled on-line with FTIR and GCMS: Thermal degradation and water adsorption capacity. *Polymer Degradation and Stability*. https://doi.org/10.1016/j.polymdegradstab.2014.12.006.

Donato, R. K., Donato, K. Z., Schrekker, H. S., & Matějka, L. (2012). Tunable reinforcement of epoxy-silica nanocomposites with ionic liquids. *Journal of Materials Chemistry, 22*(19), 9939–9948. https://doi.org/10.1039/c2jm30830d.

Fan, Y., Saito, T., & Isogai, A. (2008). Chitin nanocrystals prepared by TEMPO-mediated oxidation of α-chitin. *Biomacromolecules, 9*(1), 192–198. https://doi.org/10.1021/bm700966g.

Feng, L., Xie, N., & Zhong, J. (2014). Carbon nanofibers and their composites: A review of synthesizing, properties and applications. *Materials*. https://doi.org/10.3390/ma7053919.

Fukushima, T., Kosaka, A., Yamamoto, Y., Aimiya, T., Notazawa, S., Takigawa, T., … Aida, T. (2006). Dramatic effect of dispersed carbon nanotubes on the mechanical and electroconductive properties of polymers derived from ionic liquids. *Small, 2*(4), 554–560. https://doi.org/10.1002/smll.200500404.

Gao, Y., Jing, H. W., Chen, S. J., Du, M. R., Chen, W. Q., & Duan, W. H. (2019). Influence of ultrasonication on the dispersion and enhancing effect of graphene oxide–carbon nanotube hybrid nanoreinforcement in cementitious composite. *Composites Part B: Engineering, 164*, 45–53. https://doi.org/10.1016/J.COMPOSITESB.2018.11.066.

Gopalan Nair, K., & Dufresne, A. (2003a). Crab shell chitin whisker reinforced natural rubber nanocomposites. 1. Processing and swelling behavior. *Biomacromolecules, 4*(3), 657–665. https://doi.org/10.1021/bm020127b.

Gopalan Nair, K., & Dufresne, A. (2003b). Crab shell chitin whisker reinforced natural rubber nanocomposites. 2. Mechanical behavior. *Biomacromolecules, 4*(3), 666–674. https://doi.org/10.1021/bm0201284.

Guo, Y., Duan, B., Cui, L., & Zhu, P. (2015). Construction of chitin/graphene oxide hybrid hydrogels. *Cellulose, 22*(3), 2035–2043. https://doi.org/10.1007/s10570-015-0630-2.

Ham, Y. R., Kim, S. H., Shin, Y. J., Lee, D. H., Yang, M., Min, J. H., … Shin, J. S. (2010). A comparison of some imidazoles in the curing of epoxy resin. *Journal of Industrial and Engineering Chemistry, 16*(4), 556–559. https://doi.org/10.1016/j.jiec.2010.03.022.

Hameed, N., Salim, N. V., Hanley, T. L., Sona, M., Fox, B. L., & Guo, Q. (2013). Individual dispersion of carbon nanotubes in epoxy via a novel dispersion-curing approach using ionic liquids. *Physical Chemistry Chemical Physics, 15*(28), 11696–11703. https://doi.org/10.1039/c3cp00064h.

Ifuku, S., Nogi, M., Abe, K., Yoshioka, M., Morimoto, M., Saimoto, H., … Yano, H. (2009). Preparation of chitin nanofibers with a uniform width as α-chitin from crab shells. *Biomacromolecules*. https://doi.org/10.1021/bm900163d.

Irvin, C. W., Satam, C. C., Carson Meredith, J., & Shofner, M. L. (2019). Mechanical reinforcement and thermal properties of PVA tricomponent nanocomposites with chitin nanofibers and cellulose nanocrystals. *Composites Part A: Applied Science and Manufacturing, 116*(October 2018), 147–157. https://doi.org/10.1016/j.compositesa.2018.10.028.

Jang, M. K., Kong, B. G., Jeong, Y. I., Lee, C. H., & Nah, J. W. (2004). Physicochemical characterization of α-chitin, β-chitin, and γ-chitin separated from natural resources. *Journal of Polymer Science Part A: Polymer Chemistry, 42*(14), 3423–3432. https://doi.org/10.1002/pola.20176.

Jíšová, V. (1987). Curing mechanism of epoxides by imidazoles. *Journal of Applied Polymer Science, 34*(7), 2547–2558. https://doi.org/10.1002/app.1987.070340718.

Jun, S., Bo, K., Hong, M., Ho, W., Dye, E.Á., & Surface, Á. (2020). The effects of chitin / chitosan nanowhiskers on the thermal, mechanical and dye adsorption properties of electrospun PVA nanofibrous membranes. *Cellulose*Article 0123456789. https://doi.org/10.1007/s10570-020-03191-w.

Kadokawa, J. (2019). Dissolution, derivatization, and functionalization of chitin in ionic liquid. *International Journal of Biological Macromolecules, 123*, 732–737. https://doi.org/10.1016/j.ijbiomac.2018.11.165.

Kausar, A., & Taherian, R. (2019). *Electrical conductivity in polymer composite filled with carbon microfillers. Electrical conductivity in polymer-based composites: Experiments, modelling and applications.* Elsevier Inc.https://doi.org/10.1016/b978-0-12-812541-0.00002-1.

Kumar, A., Ghosh, P. K., Yadav, K. L., & Kumar, K. (2017). Thermo-mechanical and anticorrosive properties of MWCNT/epoxy nanocomposite fabricated by innovative dispersion technique. *Composites Part B Engineering, 113*, 291–299. https://doi.org/10.1016/J.COMPOSITESB.2017.01.046.

Kurita, K. (2001). Controlled functionalization of the polysaccharide chitin. *Progress in Polymer Science (Oxford), 26*(9), 1921–1971. https://doi.org/10.1016/S0079-6700(01)00007-7.

Li, J., Revol, J.-F., & Marchessault, R. H. (1997). Effect of degree of deacetylation of chitin on the properties of chitin crystallites. *Journal of Applied Polymer Science, 65*(2), 373–380. https://doi.org/10.1002/(sici)1097-4628(19970711)65:2 < 373::aid-app18 > 3.3.co;2-n.

Li, J., Gao, Y., Zhao, J., Sun, J., & Li, D. (2017). Homogeneous dispersion of chitin nanofibers in polylactic acid with different pretreatment methods. *Cellulose, 24*(4), 1705–1715. https://doi.org/10.1007/s10570-017-1216-y.

Liu, Y., Liu, M., Yang, S., Luo, B., & Zhou, C. (2018). Liquid crystalline behaviors of chitin nanocrystals and their reinforcing effect on natural rubber. *ACS Sustainable Chemistry & Engineering, 6*(1), 325–336. https://doi.org/10.1021/acssuschemeng.7b02586.

Liu, C., Qiu, S., Du, P., Zhao, H., & Wang, L. (2018). An ionic liquid-graphene oxide hybrid nanomaterial: Synthesis and anticorrosive applications. *Nanoscale, 10*(17), 8115–8124. https://doi.org/10.1039/c8nr01890a.

Lu, J., Yan, F., & Texter, J. (2009). Advanced applications of ionic liquids in polymer science. *Progress in Polymer Science, 34*(5), 431–448. https://doi.org/10.1016/J.PROGPOLYMSCI.2008.12.001.

Maka, H., Spychaj, T., & Pilawka, R. (2012). Epoxy resin/ionic liquid systems: The influence of imidazolium cation size and anion type on reactivity and thermomechanical properties. *Industrial & Engineering Chemistry Research*. https://doi.org/10.1021/ie202321j.

Marroquin, J. B., Rhee, K. Y., & Park, S. J. (2013). Chitosan nanocomposite films: Enhanced electrical conductivity, thermal stability, and mechanical properties. *Carbohydrate Polymers, 92*(2), 1783–1791. https://doi.org/10.1016/j.carbpol.2012.11.042.

Miyagawa, H., Misra, M., & Mohanty, A. K. (2005). Mechanical properties of carbon nanotubes and their polymer nanocomposites. *Journal of Nanoscience and Nanotechnology, 5*(10), 1593–1615. https://doi.org/10.1166/jnn.2005.181.

Morin, A., & Dufresne, A. (2002). Nanocomposites of chitin whiskers from Riftia tubes and poly(caprolactone). *Macromolecules, 35*(6), 2190–2199. https://doi.org/10.1021/ma011493a.

Moussout, H., Ahlafi, H., Aazza, M., & Bourakhouadar, M. (2016). Kinetics and mechanism of the thermal degradation of biopolymers chitin and chitosan using thermogravimetric analysis. *Polymer Degradation and Stability, 130*, 1–9. https://doi.org/10.1016/j.polymdegradstab.2016.05.016.

Nair, K. G., Dufresne, A., Gandini, A., & Belgacem, M. N. (2003). Crab shell chitin whiskers reinforced natural rubber nanocomposites. 3. Effect of chemical modification of chitin whiskers. *Biomacromolecules, 4*(6), 1835–1842. https://doi.org/10.1021/bm030058g.

Qin, Y., Lu, X., Sun, N., & Rogers, R. D. (2010). Dissolution or extraction of crustacean shells using ionic liquids to obtain high molecular weight purified chitin and direct production of chitin films and fibers. *Green Chemistry*. https://doi.org/10.1039/c003583a.

Radich, J. G., McGinn, P. J., & Kamat, P. V. (2011). Graphene-based composites for electrochemical energy storage. *The Electrochemical Society Interface, 20*(1), 63–66. https://doi.org/10.1149/2.F08111if.

Sanes, J., Saurín, N., Carrión, F. J., Ojados, G., & Bermúdez, M. D. (2016). Synergy between single-walled carbon nanotubes and ionic liquid in epoxy resin nanocomposites. *Composites Part B Engineering, 105*, 149–159. https://doi.org/10.1016/j.compositesb.2016.08.044.

Shamsuri, A. A., & Daik, R. (2015). Applications of ionic liquids and their mixtures for preparation of advanced polymer blends and composites: A short review. *Reviews on Advanced Materials Science, 40*(1), 45–59.

Shibata, M., Enjoji, M., Sakazume, K., & Ifuku, S. (2016). Bio-based epoxy/chitin nanofiber composites cured with amine-type hardeners containing chitosan. *Carbohydrate Polymers, 144*, 89–97. https://doi.org/10.1016/j.carbpol.2016.02.033.

Shibata, M., Fujigasaki, J., Enjoji, M., Shibita, A., Teramoto, N., & Ifuku, S. (2018). Amino acid-cured bio-based epoxy resins and their biocomposites with chitin- and chitosan-nanofibers. *European Polymer Journal, 98*(September 2017), 216–225. https://doi.org/10.1016/j.eurpolymj.2017.11.024.

Suo, Z. (1992). Remarks on crack-brfdgfng concepts. *Applied Mechanics Reviews, 45*(8), 355–366.

Vashchuk, A., Fainleib, A. M., Starostenko, O., & Grande, D. (2018). Application of ionic liquids in thermosetting polymers: Epoxy and cyanate ester resins. *Express Polymer Letters, 12*(10), 898–917. https://doi.org/10.3144/expresspolymlett.2018.77.

Withers, G. J., Yu, Y., Khabashesku, V. N., Cercone, L., Hadjiev, V. G., Souza, J. M., ... Davis, D. C. (2015). Improved mechanical properties of an epoxy glass–fiber composite reinforced with surface organomodified nanoclays. *Composites Part B Engineering, 72*, 175–182. https://doi.org/10.1016/J.COMPOSITESB.2014.12.008.

Wu, Q., Xie, D., Zhang, Y., Jia, Z., & Zhang, H. (2019). Mechanical properties and simulation of nanographene/polyvinylidene fluoride composite films. *Composites Part B Engineering, 156*, 148–155. https://doi.org/10.1016/J.COMPOSITESB.2018.08.061.

Wu, Y., Sasaki, T., Irie, S., & Sakurai, K. (2008). A novel biomass-ionic liquid platform for the utilization of native chitin. *Polymer, 49*(9), 2321–2327. https://doi.org/10.1016/j.polymer.2008.03.027.

Xiang, X., Suo, H., Xu, C., & Hu, Y. (2018). Covalent immobilization of lipase onto chitosan-mesoporous silica hybrid nanomaterials by carboxyl functionalized ionic liquids as the coupling agent. *Colloids and Surfaces B, Biointerfaces, 165*, 262–269. https://doi.org/10.1016/j.colsurfb.2018.02.033.

Yokoyama, T., Taft, R. W., & Kamlet, M. J. (1976). The solvatochromic comparison method. 3. Hydrogen Bonding by some 2-nitroaniline derivatives. *Journal of the American Chemical Society, 98*(11), 3233–3237. https://doi.org/10.1021/ja00427a030.

Yousfi, M., Livi, S., & Duchet-Rumeau, J. (2014). Ionic liquids: A new way for the compatibilization of thermoplastic blends. *Chemical Engineering Journal, 255*, 513–524. https://doi.org/10.1016/j.cej.2014.06.080.

Zakaria, M. R., Md Akil, H., Abdul Kudus, M. H., Ullah, F., Javed, F., & Nosbi, N. (2019). Hybrid carbon fiber-carbon nanotubes reinforced polymer composites: A review. *Composites Part B Engineering, 176*, Article 107313. https://doi.org/10.1016/J.COMPOSITESB.2019.107313.

Zhang, Q., Wei, S., Huang, J., Feng, J., & Chang, P. R. (2014). Effect of surface acetylated-chitin nanocrystals on structure and mechanical properties of poly(lactic acid). *Journal of Applied Polymer Science, 131*(2), 2–9. https://doi.org/10.1002/app.39809.

Zhou, T., Mingyuan, G. U., Jin, Y., & Wang, J. (2005). Mechanism and kinetics of epoxy-imidazole cure studied with two kinetic methods. *Polymer Journal, 37*(11), 833–840. https://doi.org/10.1295/polymj.37.833.

Zhou, T. Y., Qi, Q. Y., Zhao, Q. L., Fu, J., Liu, Y., Ma, Z., ... Zhao, X. (2015). Highly thermally stable hydrogels derived from monolayered two-dimensional supramolecular polymers. *Polymer Chemistry, 6*(16), 3018–3023. https://doi.org/10.1039/c5py00072f.